Vegetation map of Trail Valley Creek, Northwest Territories, Canada

Inge Grünberg and Julia Boike

August 21, 2019

Abstract

The vegetation map distinguishes between five tundra vegetation types, trees, and open water at the forest–tundra transition north of Inuvik, Northwest Territories, Canada. The area is underlain by continuous permafrost. Vegetation types were distinguished based on vegetation height derived from airborne laser scanning, airborne orthophotos and observations from the field site. A detailed description of the data sources and processing steps is included.

1 Technical details

Data format Geo-Tiff

Projection UTM zone 8N, WGS84

Origin 548183.5,7630973.5

Dimensions X: 1601 Y: 1489, one band

Pixel Size $10\,\text{m} \cdot 10\,\text{m}$

Data Type Sixteen bit signed integer

No-data value -9999

Data values 0: tree, 1: tall shrub, 2: riparian shrub, 3: dwarf shrub, 4: tussock, 5: lichen, 6: water

2 Study site

The vegetation map covers the Trail Valley Creek study site east of the Mackenzie Delta and 45 km north of Inuvik, Northwest Territories, Canada (rectangle of $106\,\text{km}^2$ between 133.8116 and 133.4137 °E and 68.6515 and 68.7840 °N). A detailed description of the study area can be found in Marsh et al. (2008, 2010). We classified the vegetation into six types

(tree, tall shrub, riparian shrub, dwarf shrub, tussock, and lichen tundra) and included water surfaces in the classification.

3 Data sources used

Point observations from field work at the site, photographs, and experience to judge the vegetation type on high resolution airborne orthophotos

High resolution airborne orthophotos by ESRI Satellite, GOOGLE Satellite, and the MACS camera on board of the Polar 5 air-plane 25 August 2018 (spatial resolution of 7 cm) to define the calibration and validation polygons

Airborne laser scanning data of topographic characteristics and vegetation properties acquired mid of September 2016 at the Trail Valley Creek site (Anders et al., 2018) to be used as input for the classification

Airborne orthophotos by the Northwest Territories Centre for Geomatics which were acquired in 2004–2008 with red-green-blue (RGB) bands to be used as input for the classification

4 Processing steps with QGIS 2.18

Airborne laser scanning data was processed in the following steps:

1. Download rasters derived from laser scanning data from Pangea: `https://doi.pangaea.de/10.1594/PANGAEA.894884`

2. Calculate slope, aspect, roughness, and TPI (Topographic Position Index) from the DEM (Digital Elevation Model) using the *gdaldem* functions

3. Resample the rasters from 1 m to 10 m spatial resolution using the

   - Maximum for maximum vegetation height and TPI
   - Average for mean vegetation height, slope, and elevation (only for watershed analysis)
   - Median for aspect and roughness
   - Standard deviation for TPI

4. Compute the Topographic Index using watershed analysis of the 10 m elevation

5. Create mask with the laser scanning data extent

Airborne orthophotos by the Northwest Territories Centre for Geomatics were processed in the following steps:

1. Download airborne orthophotos from the Northwest Territories Centre for Geomatics `http://www.geomatics.gov.nt.ca`

2. Clip tiles to match the DEM extent

3. Merge all tiles to one

4. Merge three bands into one raster

5. Compute Hue-Intensity-Saturation (HIS) image

Table 1: Number of polygons, total area of the polygons (m^2) and number of pixels (10 m·10 m) in the gridded dataset used for calibration and validation of the vegetation map; the areas differ slightly in the gridded version of the dataset.

	Calibration			Validation			Total		
	#	Area	Pixels	#	Area	Pixels	#	Area	Pixels
Tree	13	91117	916	14	124696	1261	27	215813	2177
Tall shrub	22	100889	1006	23	126732	1279	45	227621	2285
Riparian shrub	27	170624	1715	28	189818	1907	55	360442	3622
Dwarf shrub	28	278487	2811	29	283300	2861	57	561787	5672
Tussock	26	210803	2117	26	230173	2318	52	440976	4435
Lichen	42	75074	772	43	81034	834	85	156108	1606
Water	11	177767	1798	11	208994	2118	22	386761	3916
total	169	1104761	11135	174	1244747	12578	343	2349508	23713

6. Resample the rasters from 0.5 m to 10 m spatial resolution using the

- Average for RGB and HIS (6 bands)
- Standard deviation for RGB (3 bands)

Manual identification of vegetation reference areas was needed for calibration and validation regions. We used point observations as a basis for interpreting high resolution airborne orthophotos. In more detail, we followed the following workflow:

1. Load locations of field observations

2. Load high resolution airborne orthophotos

3. Identify polygons of distinct vegetation types within the laser scanning extent

4. Check that the polygons cover the same single vegetation type in all image sources which are not perfectly co-registered

5. Divide the complete set of 343 polygons into calibration and validation subsets based on:

    - All polygons based on field observations and pictures are used for validation
    - All polygons per vegetation type are sorted by area and alternately assigned to each subset with exceptions of the field observations
    - Guarantee that polygons in the validation subset have at least the same number and a bigger total area than in the calibration subset

6. Create raster masks of vegetation calibration and validation areas matching the extent and resolution of the other datasets

The final number and area of polygons per vegetation type in both subsets is summarized in Table 1.

5 Processing steps with Python 3.6.8

Compute extra band ratios from the topographic and optical data. In more detail, we followed the following workflow:

1. Smooth the Topographic Index map with the maximum of 9 cells
2. Add additional band with $\frac{\text{Maximum}-\text{Mean}}{\text{Maximum}+\text{Mean}}$ vegetation height (called Vegetation Height Ratio)
3. Add additional band with $\frac{\text{Roughness}-\text{Meanvegetationheight}}{\text{Roughness}+\text{Meanvegetationheight}}$ (called Height Roughness Ratio)
4. Add additional band with $\frac{\text{Intensity}-4\cdot\text{Saturation}}{\text{Intensity}+4\cdot\text{Saturation}}$ (called Intensity Saturation Ratio)

Combine the classification data from the 20 bands at 10 m by 10 m spatial resolution to a single dataset:

1. Average slope
2. Median aspect
3. Median roughness
4. Maximum TPI
5. Standard deviation of TPI
6. Topographic Index
7. Maximum maximum vegetation height
8. Average mean vegetation height
9. Average of Red
10. Average of Green
11. Average of Blue
12. Average of Hue
13. Average of Intensity
14. Average of Saturation
15. Standard deviation of Red
16. Standard deviation of Green
17. Standard deviation of Blue
18. Vegetation Height Ratio
19. Height Roughness Ratio
20. Intensity Saturation Ratio

Visually analyse the band characteristics for each vegetation type using the calibration polygons. In more detail, we followed the following workflow:

1. Extract all pixel values within the manually classified calibration areas for each vegetation type
2. Calculate statistics (5th, 10th, 25th, 50th, 75th, 90th, 95th percentile, mean, minimum and maximum) for each vegetation type and water and for each of the 20 bands

Classify the complete image using a combination of manually defined thresholds for the 20 bands to discriminate between the vegetation types and water.

Filter the classified map by replacing all vegetation patches of less than 4 pixels by the vegetation type found in most of the surrounding pixels

Compute the classification accuracy based on the calibration and the validation data and an equal amount of pixels per vegetation type, namely 834 randomly selected from all validation data and 772 pixels from the calibration data, respectively.

6 Final result

The user, producer, and final accuracy of the calibration and validation data is summarized in Tables 2 and 3, respectively. All vegetation types have a user and producer accuracy above 75% in the validation dataset and above 82% in the calibration dataset. The final map accuracy is 87.7% and 89.5%, respectively. The most similar types are tussock and lichen tundra, which are most often misclassified (Table 3).

Table 2: Confusion Matrix using the calibration data.

Predicted type / Actual type	Tree	Tall shrub	Riparian shrub	Dwarf shrub	Tussock	Lichen	Water	Sum	Producer accuracy
Tree	**0.931**	0.017	0.016	0.000	0.000	0.036	0.000	1	0.931
Tall shrub	0.034	**0.826**	0.074	0.057	0.009	0.000	0.000	1	0.826
Riparian shrub	0.021	0.039	**0.909**	0.031	0.000	0.000	0.000	1	0.909
Dwarf shrub	0.000	0.091	0.007	**0.896**	0.007	0.000	0.000	1	0.896
Tussock	0.000	0.005	0.007	0.014	**0.828**	0.146	0.000	1	0.828
Lichen	0.000	0.003	0.004	0.000	0.115	**0.878**	0.000	1	0.878
Water	0.000	0.001	0.005	0.000	0.000	0.000	**0.994**	1	0.994
Sum	0.986	0.982	1.021	0.999	0.959	1.061	0.994	7	
User accuracy	0.945	0.842	0.891	0.898	0.864	0.828	1.000		**0.895**

According to the final vegetation map, tussock tundra covers the largest area within the study region (37.0%), followed by dwarf shrub (23.9%), riparian shrub (13.6%), tall shrub (10.9%) and lichen tundra (10.4%) (Table 4). Lakes cover roughly 2.4% of the area and trees grow on 1.9%. However, these values can only serve as first estimate as they are sensitive to the applied thresholds. The final vegetation map is shown completely in Figure 1 and as a detail including the most important input data in Figure 2.

While the quantitative map quality is very good (accuracy of 87.7% for validation data, each class better than 75%), a careful observer can identify some areas where the classification does not provide good results:

Other surfaces than the seven classes can be found in the study area, in particular a few man-build structures (a road and a field camp with instrumented towers) and

Table 3: Confusion Matrix using the validation data.

Predicted type / Actual type	Tree	Tall shrub	Riparian shrub	Dwarf shrub	Tussock	Lichen	Water	Sum	Producer accuracy
Tree	**0.860**	0.080	0.023	0.000	0.013	0.024	0.000	1	0.860
Tall shrub	0.110	**0.819**	0.064	0.006	0.000	0.001	0.000	1	0.819
Riparian shrub	0.062	0.008	**0.929**	0.000	0.000	0.000	0.000	1	0.929
Dwarf shrub	0.000	0.020	0.000	**0.927**	0.050	0.002	0.000	1	0.927
Tussock	0.000	0.006	0.011	0.037	**0.814**	0.132	0.000	1	0.814
Lichen	0.000	0.001	0.001	0.002	0.201	**0.794**	0.000	1	0.794
Water	0.001	0.000	0.005	0.000	0.000	0.000	**0.994**	1	0.994
Sum	1.034	0.935	1.032	0.972	1.079	0.953	0.994	7	
User accuracy	0.832	0.876	0.900	0.953	0.754	0.833	1.000		**0.877**

disturbed areas with bare soil or grass and sedge dominated vegetation. These surface types are very limited in area and were not considered in the classification. They also change more rapidly than the landscape in general. However, these areas were not excluded but misclassified.

Small scale patterns cannot be resolved in the vegetation map of 10 m spatial resolution. This is in particular a problem in polygonal areas which show small scale differences between open water, sedges, shrubs on rims, and/or lichen vegetation in dry centres. In the map, polygonal areas are typically classified as lichen or tussock tundra or as riparian shrubs.

Small patches of trees in riparian and tall shrub areas are unlikely at the study site and thus usually a result of misclassification. These are likely a result of very tall vegetation, as everything above 3 m is defined as tree. While shrubs of this size are indeed unlikely, it may well be that the LiDAR vegetation height is not accurate in areas of steep slopes, deeply incised channels and at densely vegetated lake shores. In general, such small patches should correctly be classified as tall shrub or riparian shrub.

Lichen and tussock tundra are more often mixed up than other classes. The main reason is that both types appear bright on the orthophotos and vegetation heights below 30 cm are not properly resolved in the LiDAR data. The DEM is also too coarse to resolve the small scale hummocks.

Vegetation islands in lakes occur in a few cases if the LiDAR derived DEM has a higher roughness than expected for an open water surface or if the orthophotos are unusually bright because of reflections on the water surface.

These known issues could be improved by using orthophotos and airborne LiDAR of higher spatial resolution. To properly solve all problems, a manual postprossessing including an assessment of each vegetation patch would be necessary.
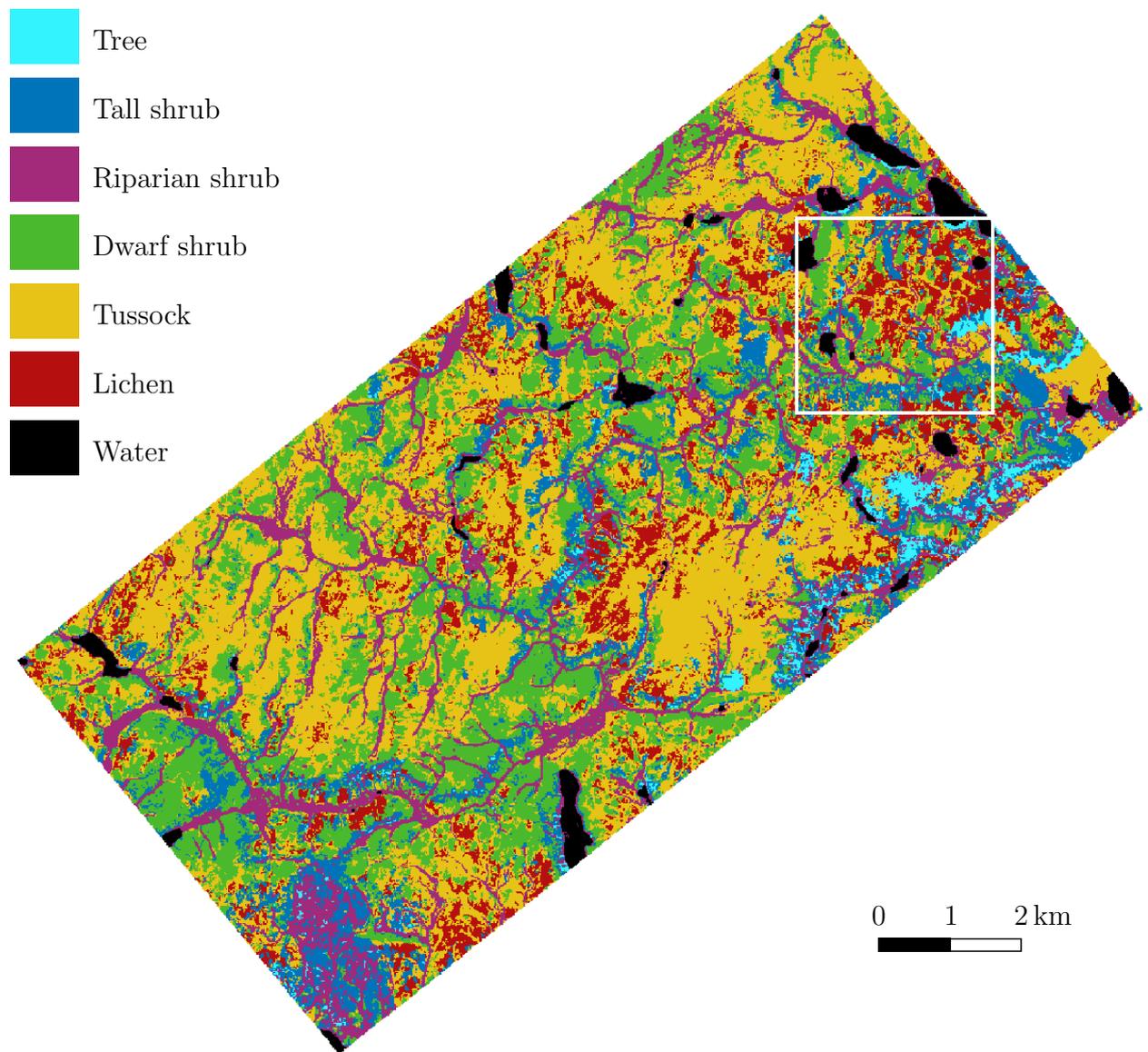
Figure 1: Final vegetation map in its complete extent; the white square indicates the extent shown in Figure 2.
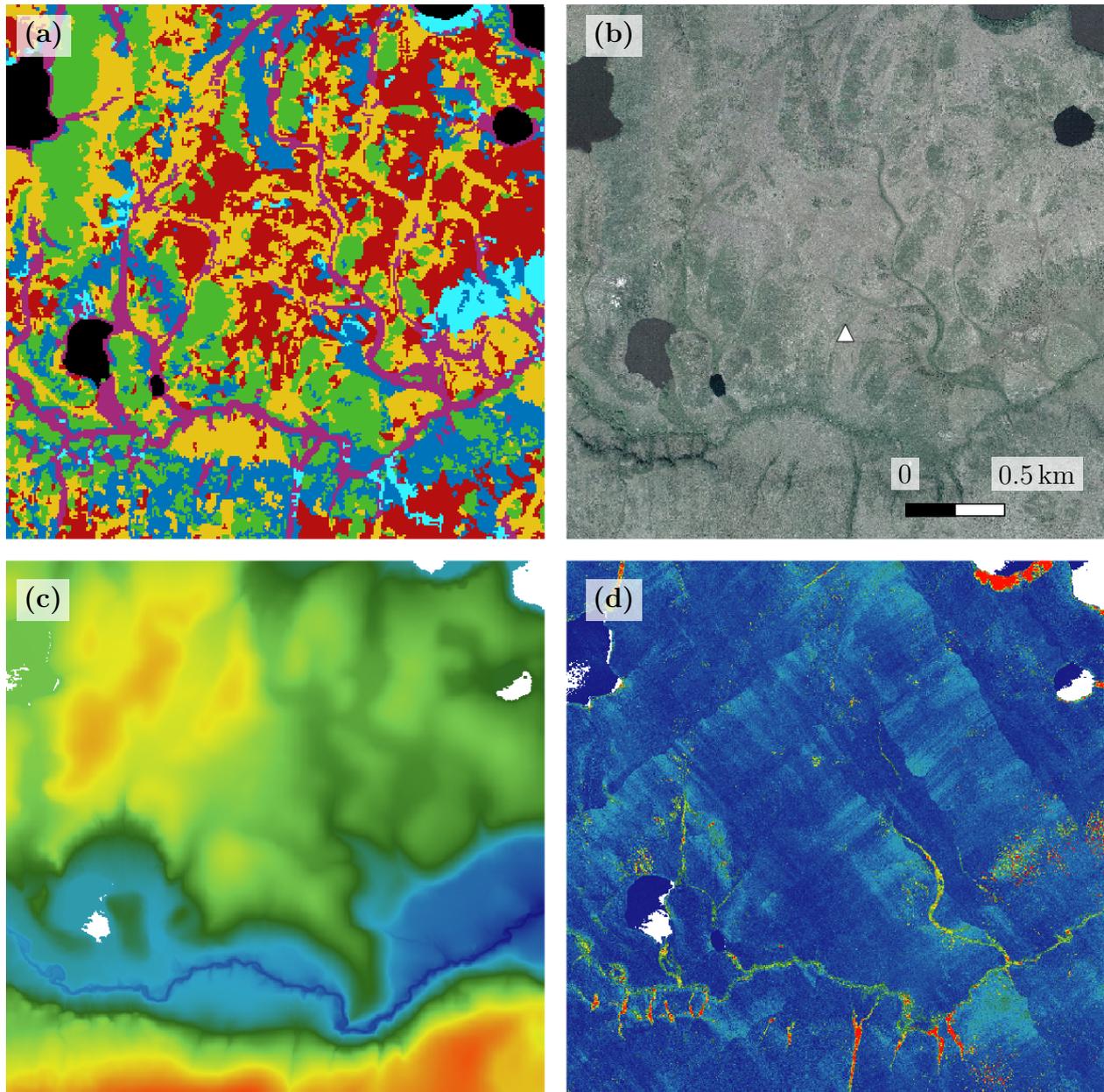
Figure 2: (a) Detail of the final vegetation map (please see legend in Figure 1) and examples of the input data: (b) airborne orthophotos from the Northwest Territories Centre for Geomatics, the white triangle indicates the location of the Trail Valley Creek Camp, (c) digital elevation model obtained from airborne laser scanning data (the colour scale is dark blue: 40 m to red: 120 m) and (d) maximum vegetation height obtained from airborne laser scanning data (the colour scale is dark blue: 0 m to red: ≥2 m).

7 Explanation of the classification approach

We used **supervised classification** instead of clustering approaches because we needed to be able to relate the classes to specific vegetation types observed in the field. The main aim of our study was to provide a basis for potential upscaling approaches.

We used **manually defined thresholds** to distinguish between different vegetation types and water. This is in contrast to often used other approaches such as Maximum Likelihood Classification or more recent tools of machine learning such as Random Forest. We compared our results to the output of several machine learning techniques using the default parameters of the implementation in the Python 3 sklearn package, namely *Decision Tree*, *Extra Trees*, *K Neighbors*, *Linear Regression*, *Logistic Regression*, *Gaussian Naive Bayes*, *Linear Discriminant Analysis*, *Quadratic Discriminant Analysis*, *Random Forest*, *Gradient Boosting*, *Ada Boost*, and *Bagging*. Most algorithms yielded worse results for overall accuracy, minimum user and/or minimum producer accuracy as compared to the simple thresholds approach. We only got better results using *Extra Trees*, *Decision Tree*, *Gradient Boosting*, and *Gaussian Naive Bayes*. However, we decided to use the more simple approach because (I) the improvement in accuracy of the validation data was only moderate, up to 6% for the final accuracy, (II) the choice of parameters, the specific implementation and, in some cases, the random nature of the approaches yield less reproducible results, and (III) it is much more challenging to understand why certain results were obtained and why the approach works better or worse in specific cases.

However, we used the machine learning results of the well-fitted models to assess whether the cover fractions of the different vegetation types were realistic. We found that our final vegetation map likely underestimates the cover fraction of trees and tall shrubs, while the area covered by riparian shrubs and dwarf shrubs is probably slightly overestimated (Table 4).

Table 4: Cover of each vegetation type according to the final vegetation map and the minimum, mean and maximum values of the four best machine learning (ML) approaches.

Vegetation type	Cover (%)			
	Final map	Minimum ML	Mean ML	Maximum ML
Tree	1.9	3.0	3.8	4.7
Tall shrub	10.9	15.3	16.5	17.5
Riparian shrub	13.6	8.5	10.2	12.0
Dwarf shrub	23.9	15.7	18.4	19.8
Tussock	37.0	34.8	37.2	39.7
Lichen	10.4	9.7	11.8	14.0
Water	2.4	1.9	2.1	2.2

We **filtered the final map** and added all patches with less than four pixels to a surrounding bigger patch. This processing step leads to the loss of information on small patches. We decided to use the filtering because (I) it improved the overall accuracy from 83.4% to 87.7% for the validation data and (II) visual inspection of the final map suggested that most of the small patches did not correspond to different types.

Acknowledgments

References

Anders, K., Antonova, S., Boike, J., Gehrmann, M., Hartmann, J., Helm, V., Höfle, B., Marsh, P., Marx, S., and Sachs, T.: Airborne Laser Scanning (ALS) Point Clouds of Trail Valley Creek, NWT, Canada (2016), doi:10.1594/PANGAEA.894884, 2018.

Marsh, P., Pomeroy, J., Pohl, S., Quinton, W., Onclin, C., Russell, M., Neumann, N., Pietroniro, A., Davison, B., and McCartney, S.: Snowmelt Processes and Runoff at the Arctic Treeline: Ten Years of MAGS Research, pp. 97–123, Springer Berlin Heidelberg, Berlin, Heidelberg, doi:10.1007/978-3-540-75136-6_6, 2008.

Marsh, P., Bartlett, P., MacKay, M., Pohl, S., and Lantz, T.: Snowmelt energetics at a shrub tundra site in the western Canadian Arctic, Hydrological Processes, 24, 3603–3620, doi:10.1002/hyp.7786, 2010.